Acta Materialia Transylvanica 8/1. (2025) 28–33.
DOI: Hungarian: https://doi.org/10.33923/amt-2025-01-06
English: https://doi.org/10.33924/amt-2025-01-06

ACTA MATERIALIA TRANSYLVANICA

Effect of Laser Surface Hardening on Different Surface Designs in the Case of 1.2379 Tool Steel

Béla MÉSZÁROS,[1] Enikő Réka FÁBIÁN[2]

[1] *Óbuda University, Doctoral School on Materials Sciences and Technologies, Budapest, Hungary*
meszaros.bela@bgk.uni-obuda.hu

[2] *Óbuda University, Bánki Donát Faculty of Mechanical and Safety Engineering, Institute of Materials and Manufacturing Sciences, Department of Material Technology. Budapest, Hungary*
fabian.reka@bgk.uni-obuda.hu

Abstract

Laser surface treatments are increasingly used for the formation of hardened layers. In this experimental series, we examined surfaces machined to three different depths (0.25 mm, 0.5 mm, and 0.75 mm) to determine how these machining depths affect the thickness of the hardened layer. The base material was 1.2379 tool steel in all cases. The focal distance remained constant, while the laser power and scanning speed were varied according to the predefined experimental design. Our results indicate that higher specific power led to a deeper hardened layer. The 45° machining angle—and consequently, the 45° laser beam incidence angle—enhanced absorption and increased the hardening depth. The deepest grooves resulted in the thickest hardened layer. However, during our experiments, certain parameter settings raised the base material's temperature above the liquidus point, causing localized melting.

Keywords: *tool steel, laser beam hardening, diode laser, surface texture.*

1. Introduction

Diode laser heat treatment plays an increasingly important role in surface hardening within industry, particularly in the automotive, aerospace, and tool manufacturing sectors. The principle of the process is that the laser beam provides localised heat input, which induces a martensitic transformation on the workpiece surface, thereby enhancing wear resistance and service life.

However, the energy absorption and reflection of material surfaces with different topographies have a significant impact on the quality and depth of the hardened layer. Part of the laser radiation is absorbed by the surface of the workpiece, while the remaining portion is reflected, resulting in energy loss. The degree of reflection depends on the wavelength of the applied radiation and on the surface roughness of the workpiece [1]. Due to high reflection, part of the laser radiation cannot be utilised, which may lead to uneven heat input and an inhomogeneous hardened layer. To address this issue, various industrial surface treatment techniques are applied:

- Surface oxidation: A thin oxide layer (e.g. produced by heat treatment or chemical processes) reduces reflection, particularly on polished surfaces.
- Blasting or etching: Producing a rougher surface increases absorbed energy and decreases reflection.
- Application of graphite or paint coatings: These materials improve absorptivity and are frequently used in industry prior to laser welding and surface treatments [2].

The different types of lasers operate at different wavelengths, and these operating ranges alter the amount of heat introduced into the material, thereby influencing the thickness of the hardened layer. Table 1 shows the percentage absorption capacity of different surfaces, i.e. their energy absorptivity, for two types of lasers.

The CO_2 laser operates in the infrared range (at a wavelength of 10.6 µm), while the YAG laser typically operates in the near-infrared range (at a wavelength of 1.06 µm). This difference in wave-

Table 1. *Absorption coefficient at different surface qualities and laser technologies* [3]

Surface	Absorption, %
	Diode laser, 700–1070 nm
Polished	30–40
Ground	45–55
Turned	55–65
Sandblasted	75–85
Oxidised	85–95
Graphite-coated	90–98

length plays a decisive role in how various materials and surface structures absorb laser radiation. In the case of smooth, polished surfaces, absorption is generally lower, whereas roughened or oxidised surfaces tend to absorb more energy. Regarding absorption parameters, CO_2 and YAG lasers behave differently on differently treated surfaces. For polished surfaces, absorption is low for both types of lasers, but YAG laser radiation is absorbed somewhat more effectively by metals, while CO2 laser radiation is more prone to reflection. Ground and turned surfaces already show higher absorption, particularly with the YAG laser, as the fine roughness facilitates energy absorption. Sandblasted and oxidised surfaces exhibit significantly better absorptivity for both lasers, but again the YAG laser proves more efficient. Graphite-coated surfaces demonstrate outstanding absorption in the case of both types of lasers [3].

Based on the absorption values, the YAG laser is more suitable for surface hardening, as its radiation is absorbed more effectively on various metallic surfaces, particularly on oxidised, sandblasted, and graphite-coated layers. The CO_2 laser, on the other hand, is more ideal for non-metallic materials and for the heat treatment of larger surfaces. The proper selection of the laser type therefore plays a critical role in achieving optimal heat input and uniform hardening depth.

Diode lasers are widely used laser types, applied in industrial machining, medical devices, and communication systems. These lasers operate within the 700–1070 nm wavelength range, which allows their radiation to be absorbed efficiently by various metallic surfaces, particularly when the surface is oxidised or roughened. In this experimental series, a diode laser was employed, the main advantages of which are its high mobility, ease of operation, and tunability. Table 2 presents the absorption characteristics of diode lasers on different surfaces, expressed as percentages.

Table 2. *Variation of the hardened layer thickness with laser beam incidence angle* [2]

Incidence angle	Hardened layer thickness (mm)
90°	1.2 mm
60°	0.8 mm
45°	0.5 mm

The 1.2379 steel (AISI D2) is a cold-work tool steel, for which hardening is essential to increase service life and wear resistance. During diode laser surface hardening, the thickness of the hardened layer typically varies between 0.3 and 1.5 mm, depending on the laser power and the machining speed [4]. The thickness of the hardened layer also depends on additional factors, such as the angle of incidence of the beam. This determines energy absorption and heat distribution. A 90° incidence angle ensures optimal absorption, whereas at smaller angles (e.g. 45°) part of the radiation is deflected from the surface, reducing the efficiency of hardening [5].

In an experiment, diode laser surface hardening of AISI 410 stainless steel was examined at different incidence angles, where the hardened layer thicknesses obtained are shown in Table 2, in accordance with the angle of incidence of the beam.

2. Materials, equipment and technologies

The base material was a Ø80 mm hot-rolled, pre-hardened 1.2379 (X153CrMoV12 or D2) tool steel bar (1.53% C, 0.35% Si, 0.4% Mn, 12% Cr and 0.85% V), with a hardness of HB 230–250. For the experiments, slices of 30 mm thickness were cut, and the plane surfaces thus obtained were used for the tests. In order to determine how machining surfaces influence laser hardening, V-shaped grooves of different depths were produced.

Surface preparation of the specimens was carried out on a universal milling machine, where grooves of 0.25, 0.5 and 0.75 mm depth were milled (see Fig. 1). The tool applied was a solid carbide end mill (MC326-12.0W4L050C-WK-40TF) with a main cutting edge angle of 90°. The V-shaped grooves were created by tilting the main spindle and owing to the design of the tool, while an appropriate coolant-lubricant was applied. During the milling operations, ensuring

proper cooling and lubrication was essential for maintaining the quality of the machining process.

Laser heat treatment was carried out at the laser technology plant of Budai Benefit Kft. During the process, a 4 kW diode laser was applied with three different sets of technological parameters.

The aim of the procedure was to investigate the effect of grooves of different depths on laser heat treatment and on the properties of the material. The experimental results contribute to determining the optimal technological parameters for industrial applications. Based on preliminary literature research [2, 6] the specimen surfaces were scanned with specific heat inputs of 150, 200 and 240 Ws/mm. During the surface treatment, a focal distance of 340 mm was used, measured relative to the plane surfaces. The technological data belonging to each specimen designation are shown in Table 3.

The surface-treated specimen was cut 10 mm away from the heat-treated surfaces using a band saw with the application of coolant-lubricant (see Fig. 2). From the resulting plates, strips of 40 mm width were sectioned along the centreline of the heat-treated tracks for metallographic examinations, ensuring that the specimens contained evaluable portions both from the grooved area and from the plane surface.

After cold mounting, the specimens were ground and polished in several stages, and then etched with Nital-2 in order to reveal the hardened layer thicknesses. The optical microscopic analyses were performed using an Olympus DSX1000 digital microscope.

The hardness of the specimens was measured with a Zwick 3212 hardness tester, both perpendicular to the plane surface and starting from the tip of the grooves. In order to measure hardness variations while maintaining the prescribed spacing between indentations [7], the applied load was selected as 1.962 N.

3. Experimental results

Our conclusions were drawn from microscopic analyses of the prepared cross-sections and from the hardness profiles measured on the specimens.

The preliminary literature research [6], and the metallographic examinations show that the thickness of the hardened layer is smaller than at the machined surfaces. It can be observed that even at the lowest specific energy input, the sharp peaks and valleys of the machined V-shaped grooves lost their form, and rounded shapes began to appear (Fig. 3). The originally produced shape is indicated by a red line in Fig. 3. In this experimental series, this setting represented the condition where the least amount of heat was introduced into the base material.

Table 3. *Technological data for each specimen*

Set parameters	Specimen number and corresponding machining depth		
	0.25 mm	0.5 mm	0.75 mm
1.2 kW → 8 mm/s	22	23	24
1.6 kW → 8 mm/s	25	26	27
1.2 kW → 5 mm/s	28	29	30

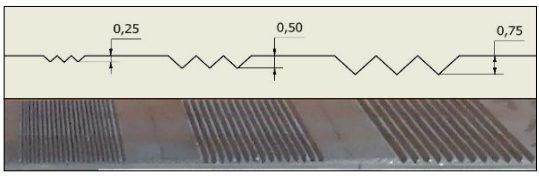

Fig. 1. *Schematic and image of the prepared surfaces.*

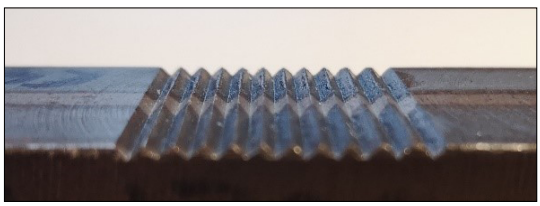

Fig. 2. *Grooves of 0.75 mm depth after heat treatment.*

To reveal the hardness variation, hardness measurements were performed both perpendicular to the plane surface and starting from the edges of the machined grooves. Based on the data thus obtained, hardness variation diagrams were constructed.

The highest hardness values were typically measured in the hardened surface layer, gradually decreasing towards the core. The hardness measurement results obtained with the lowest heat input are shown in Fig. 4.

The hardness measurements show that at the machined peaks the hardness of the hardened layer is higher than in the vicinity of the plane surface. This indicates that greater heat absorption occurred at the machined edges, which may have contributed to the increase in primary aus-

Fig. 3. *Effect of surface heat treatment with a specific heat input of 150 Ws/mm on specimen 22.*

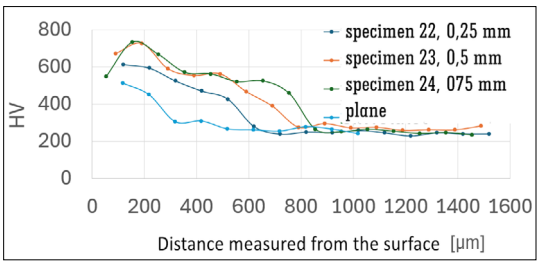

Fig. 4. *Hardness variation after heat treatment with a specific heat input of 150 Ws/mm.*

tenite grain size. The hardness measurement results (**Fig. 4**) also reveal that, in specimens with deeper grooves, the hardness close to the surface at the machined peaks is lower than at 200 µm from the surface, a phenomenon that is also reflected in the microstructure (**Fig. 5**).

In the next experimental setting, the laser power was increased from 1200 W to 1600 W, while the scanning speed was kept constant (8 mm/s). As a result of this adjustment, the specific heat input increased to 200 Ws/mm compared with the previous setting. Metallographic examinations revealed that the peaks formed by machining became rounded and partially melted. At low magnification, following etching with Nital, the melted and resolidified regions appear bright (**Fig. 6**). At higher magnification, dendritic solidification is also clearly visible (**Fig. 7**). Beneath the melted regions, two transitional zones can be identified. Directly under the melted zone, a region can be observed where the temperature rose between the solidus and Acm, in which homogenisation of the original carbide network structure began. However, due to the short duration of surface treatment, the microstructure did not become homogeneous. In the central region shown in **Fig. 6** heating occurred between A1 and Acm, and due to rapid cooling of the specimen, martensitic transformation took place in the areas between the carbide networks. This conclusion is supported by the hardness measurement results shown in **Fig. 8.** At a depth of 400–600 µm from the surface, the material hardness reached values of

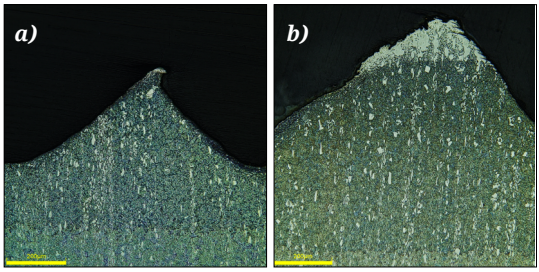

Fig. 5. *Vicinity of the machined peak after surface treatment. a) specimen 22 b) specimen 24.*

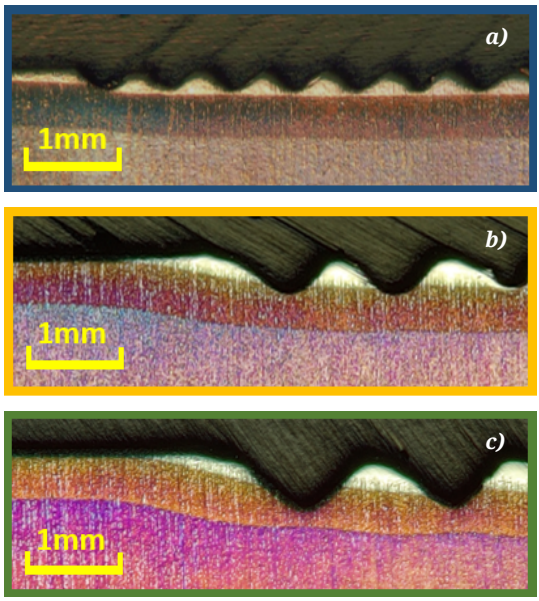

Fig. 6. *Cross-sectional appearance of surface heat treatment with a specific beam energy of 200 Ws/mm a) specimen 25 b) specimen 26 c) specimen 27.*

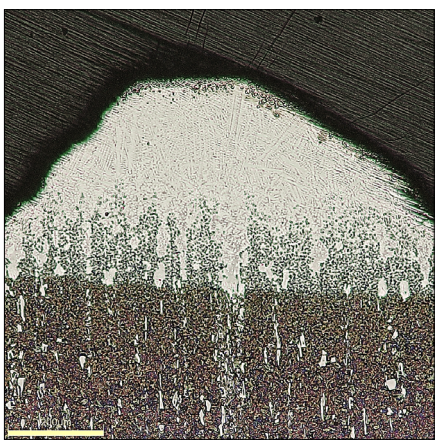

Fig. 7. *Vicinity of the machined peak after surface treatment. Specimen 26.*

700–750 HV in the grooved regions of 0.5 mm and 0.75 mm depth..

In our final measurement series, we applied a scanning speed of 5 mm/s to the original power of 1200 W, thereby further increasing the specific heat input, so that the plane surface was exposed to a radiation energy of 240 Ws/mm. In this case, the amount of heat transferred into the surface of the base material was sufficient to melt it at the machined peaks (Fig. 9), Consequently, the hardness of the material at these locations was significantly lower than in the regions where only surface hardening occurred, as illustrated in Fig. 10.

The hardness variation diagrams show that in the near-surface region the hardness starts at 500 HV, and as the distance from the surface increases, a harder layer (800 HV) forms at a depth of 450 µm (Fig. 10).

Fig. 9. clearly demonstrates that due to the applied heat input the sharp corners melted, resulting in completely distorted, rounded shapes in the profile.

Inappropriate selection of parameters during the heat treatment of the base material may even cause melting, which, in addition to leading to inadequate surface hardness and wear resistance, can also deform the machined edges—a factor that results in non-conformity in the case of a cold-working tool.

4. Conclusions

In our laser hardening experiments, the behaviour of 1.2379 cold-work tool steel was examined under three different settings with various surface designs. In all cases, the deepest machining depth (0.75 mm) resulted in the deepest hardened layer. The thinnest hardened layer was consistently formed on the plane surface. A laser beam incidence angle of 45° produced higher heat input than perpendicular irradiation.

Where localised melting occurred near the surface due to the surface geometry of the product, dendritic crystallisation developed. The hardness in these regions was lower than in areas where only a martensitic heat-treated microstructure was formed.

For diode laser heat treatment of 1.2379 tool steel, machining depths of 0.5 mm with a 45° inclination still produced a homogeneous hardened layer at a power of 1200 W and a scanning speed of 8 mm/s. At higher energy inputs, however, surface melting may occur, particularly in the vicinity of carbide networks.

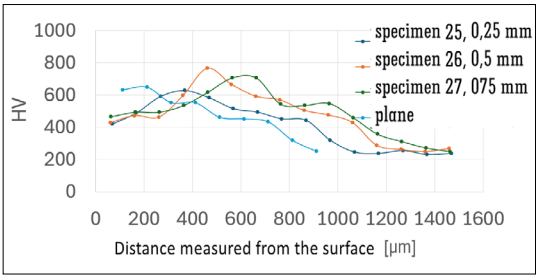

Fig. 8. *Hardness profiles after heat treatment with a specific energy of 200 Ws/mm.*

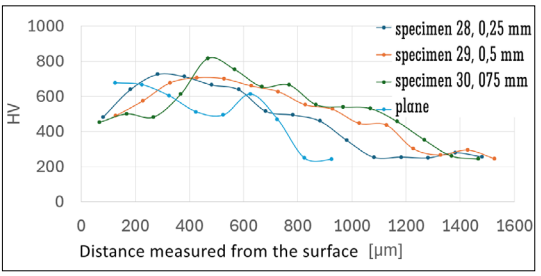

Fig. 9. *Hardness profiles after heat treatment with a specific heat input of 240 Ws/mm.*

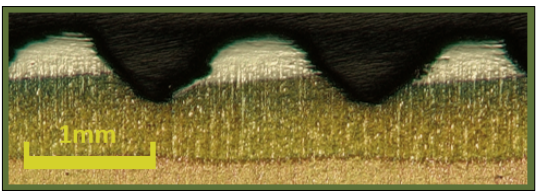

Fig. 10. *Cross-sectional appearance of surface heat treatment with a specific heat input of 240 Ws/mm, specimen 30.*

References

[1] Henrikki P., Veli K.: *Diode laser beam absorption in laser transformation hardening of low alloy steels*. Journal of Laser Applications, 16/3. (2004) 147–153. https://doi.org/10.2351/1.1710879

[2] Moradi M., Arabi H., Jamshidi N, Benyounis K.: *A comparative study of laser surface hardening of AISI 410 and 420 martensitic stainless steels by using diode laser*. Optics & Laser Technology, 111. (2019) 347–357. https://doi.org/10.1016/j.optlastec.2018.10.013

[3] Buza G: *Lézersugaras technológiák I.* Kézirat. Edutus Főiskola, Tatabánya, 2012.

[4] Temmler A., Cortina M., Ross I., Küpper M. E., Rittinghaus S. K.: *Evolution of Surface Topography and Microstructure in Laser Polishing of Cold Work Steel 1.2379 (AISI D2) Using Quadratic, Top-*

Hat Shaped Intensity Distributions. Materials, 15/3. (2022) 769. https://doi.org/10.3390/ma15030769

[5] Dewi H. S., Volp J., Kaplan A. F. H.: *Leaser beam absorbtion depending on the angle of incidence on groud surfaces.* Laser in manufacturing conference LIM 2019. 1–6. pdf.

[6] Mészáros B., Fábián E. R.: *The Effect of Surface Machining Design on the Efficiency of Laser Surface Treatment.* Acta Materialia Transylvanica, 7/2. (2024) 88–93. https://doi.org/10.33924/amt-2024-02-06

[7] MSZ EN ISO 6507-1:2024 Fémek. Vickers-keménységmérés. Mérési eljárás, 2024.